Scripta Materialia 108 (2015) 88–91

Contents lists available at ScienceDirect

Scripta Materialia

journal homepage: www.elsevier.com/locate/scriptamat

Asymmetry in steel welds with dissimilar amounts of sulfur

H.L. Wei [a], S. Pal [a], V. Manvatkar [a], T.J. Lienert [b], T. DebRoy [a,*]

[a] Department of Materials Science and Engineering, The Pennsylvania State University, 309 Forest Resources Lab, University Park, PA 16802, USA
[b] Materials Science Division, Los Alamos National Laboratory, PO Box 1663, Los Alamos, NM 87545, USA

ARTICLE INFO

Article history:
Received 22 May 2015
Revised 12 June 2015
Accepted 15 June 2015
Available online 16 June 2015

Keywords:
Surface active element
Center line shift (CLS)
Marangoni flow

ABSTRACT

During welding of steels containing dissimilar amounts of sulfur, the weld pool is shifted laterally from the original joint interface and rotated at an angle with the interface. The mechanism for this unusual behavior is not known. Here, we show for the first time through comparison of numerically calculated and experimental results that Marangoni convection causes these rotational and translational asymmetries and the reported arc shift is a consequence of asymmetric melting rather than its cause.

When two steel plates containing dissimilar concentrations of sulfur are arc welded, a very unusual and strikingly asymmetric weld pool geometry forms [1,2]. When the arc is initially placed directly above the original interface of the two plates, the lower sulfur containing plate melts to a much greater extent than the higher sulfur plate and the maximum penetration does not occur at the expected plane of original interface between the two plates [1,2]. Instead, its location is shifted away from the interface well within the low sulfur containing plate and pronounced preferential melting of the low sulfur steel plate takes place. Extensive experiments and modeling have suggested that the effect is caused by a combination of both a lateral shift of the arc from its original location above the butting surface and a net transport of the hot liquid alloy from the high sulfur steel to the low sulfur steel by Marangoni convection [2]. The pronounced effect of sulfur on the convection pattern and the resulting shape and size of the weld pool is well recognized in the literature [3–9]. Evidence of arc asymmetry was observed during the experiments [2,10] and is not unexpected. The welding arc is known to be stabilized by metal vapors. Since the melting occurs preferentially in the low sulfur plate, it is conceivable that more metal vapors are present above the low sulfur plate and the arc asymmetry may be a consequence rather than the driver of the preferential melting of the low sulfur plate. One way to address this question is to avoid the arc altogether and thus avoid any preferential melting contributed by the arc shift.

In a recent paper, we reported experimental results of laser beam welding of austenitic stainless steels containing dissimilar amounts of sulfur [1]. Since laser beams can be precisely positioned and their position remains unaffected by metal vapors, these experiments avoided uncertainties in the location of the heat source. In these experiments, a pronounced center line shift (CLS), measured by a lateral shift of the location of the maximum penetration depth away from the joint interface, was accompanied by a definitive and reproducible rotational asymmetry (RA) of the weld pool geometry [1]. The presence of CLS and RA in the absence of any arc shift clearly indicates the need to examine Marangoni convection as the sole cause of the uneven melting of the work pieces and the observed rotational asymmetry of the laser weld pool. Such an investigation can provide a definitive proof of the underlying scientific reason for CLS and RA.

Here we report numerical simulation of heat transfer and liquid metal flow during laser welding of dissimilar sulfur containing steel welds in transient, three dimensional form. A comprehensive numerical model has been developed and tested to study the temperature and the velocity fields in the weld pool during welding of the two austenitic stainless steel plates with dissimilar concentrations of sulfur. The compositions of the two steels are shown in Table 1. The mathematical model solves the equations of conservation of mass, momentum and energy with a sub-model for temperature and composition dependent surface tension of steel [11,12]. By comparing the simulated geometrical features of fusion zone size, CLS and RA, the mechanism of formation of CLS and RA can be elucidated definitively.

In the computational domain, each plate was 70 mm long, 20 mm wide and 8 mm deep. It was divided into 114 grid points in welding direction (x), 94 in transverse direction (y) and 40 in the thickness (z) direction. The local values of the variables of each

* Corresponding author.
E-mail address: debroy@psu.edu (T. DebRoy).

http://dx.doi.org/10.1016/j.scriptamat.2015.06.024
1359-6462/

Table 1
Compositions of 303 and 304 L stainless steels (wt%).

SS	S	C	P	Si	Mn	Cr	Ni	Mo	N	Cu
303	0.293	0.050	0.027	0.510	1.620	17.210	8.720	NA	NA	NA
304 L	0.003	0.022	0.028	0.303	1.811	18.537	8.453	0.296	0.052	0.246

computational cell are related to the variable values of the neighboring cells with algebraic equations [13]. The numerical model developed in the work was similar to that described in our previous work [2,14,15] except a transient term was added in each of the mass, momentum and energy conservation equations. The equations of conservation of mass, momentum and energy were discretized for three components of velocities, pressure, sulfur concentration, and enthalpy. For the grid used, the discretization resulted in $114 \times 94 \times 40$ equations each for the six variables per iteration per time step. At a given time step during each iteration, approximately 2.6 million discretized equations were solved by tri-diagonal matrix algorithm which is a version of the Gaussian elimination technique. A description of the governing equations, boundary conditions, and the algorithm used is available in our previous papers [2,14,15] and is not repeated here. The time step was varied to obtain the computed values of temperatures and velocities independent of the time step and a time step of 0.05 s was found to be appropriate.

The accuracy of the numerical solution was evaluated by measuring the imbalance of mass, momentum and enthalpy in every cell. Iterations were conducted until the largest mass, momentum and enthalpy imbalance in any cell was smaller than a small fraction of the inlet mass, momentum and energy in the cell. This fraction was set at 10^{-6}, 10^{-5} and 10^{-3} for enthalpy, mass and momentum equations, respectively. In addition, an overall heat balance in the entire domain was examined and the total heat input was required to be within 0.5% of sum of the heat loss and accumulation values. The calculated values of velocities, weld pool dimensions and the temperature fields were found to reach a steady state after about 4.5 s. The data used for the calculations is given in Table 2. The computed weld pool profile was then used to estimate the rotational and translational asymmetries of the weld pool. The translational asymmetry (TA) of the melt pool is expressed as

$$\mathrm{TA} = 100 \times \Delta W / W \tag{1}$$

where ΔW is the difference in the widths of the molten regions in the two plates and W is the total width of the weld pool. The rotational asymmetry (RA) of the welding is expressed as:

$$\mathrm{RA} = \theta \tag{2}$$

where θ is equal to the angle of rotation of the weld pool major axis with respect to the laser welding direction.

Fig. 1 shows both the metallographic transverse weld section obtained from the experiment [1] and the calculated weld cross section with temperature and velocity fields by the fluid flow and heat transfer model. In the computed results, the solidus line is indicated as the 1673 K isotherm which is the boundary of the weld pool. It can be observed that the position of the maximum penetration does not coincide with the original interface of the two plates. The location of the maximum penetration is shifted toward the low sulfur region. The computed value of this center line shift (CLS) of maximum penetration location is 0.79 mm and the corresponding experimentally measured CLS is 0.8 mm. Fig. 1 shows that the computed weld cross section profile and dimensions agrees well with experimentally determined weld.

Previous reports have shown that the temperature coefficient of surface tension can be significantly affected by the presence of sulfur in steels. The direction and magnitude of Marangoni stress can be altered, resulting in different flow patterns of the liquid weld metal [7,11] when sulfur is present. The calculated velocity field of the molten pool demonstrates that starting from the high sulfur piece periphery, the Marangoni convection flows inward to the joint interface. Part of the molten metal flows back and forms one circulation cell on the high sulfur side. Another portion of molten metal continues to flow through the joint interface, heading towards the low sulfur side. Large amounts of heat are transported by this particular fluid flow pattern from the high sulfur to the low sulfur piece. Consequently, an asymmetric transverse weld section

Table 2
Data used for numerical calculations.

Property parameters	Value
Laser power (W)	2000
Laser beam radius (mm)	1.5
Welding Speed (mm s^{-1})	2.12
Liquidus temperature (K)	1727
Solidus temperature (K)	1673
Density of metal (kg m^{-3})	7200
Thermal conductivity of solid (J m^{-1} s^{-1} K^{-1})	16.74
Effective thermal conductivity of liquid (J m^{-1} s^{-1} K^{-1})	21.76
Specific heat of solid (J kg^{-1} K^{-1})	661.1
Specific heat of liquid (J kg^{-1} K^{-1})	808.05
Temperature coefficient of surface tension (N m^{-1} K^{-1})	-0.4×10^{-3}
Coefficient of thermal expansion (K^{-1})	1.0×10^{-5}
Effective viscosity of liquid (kg m^{-1} s^{-1})	0.014
Surface excess of sulfur at saturation (mol m^{-2})	1.3×10^{-5}
Enthalpy of segregation (J mol^{-1})	-1.66×10^{5}
Entropy factor	0.318×10^{-3}

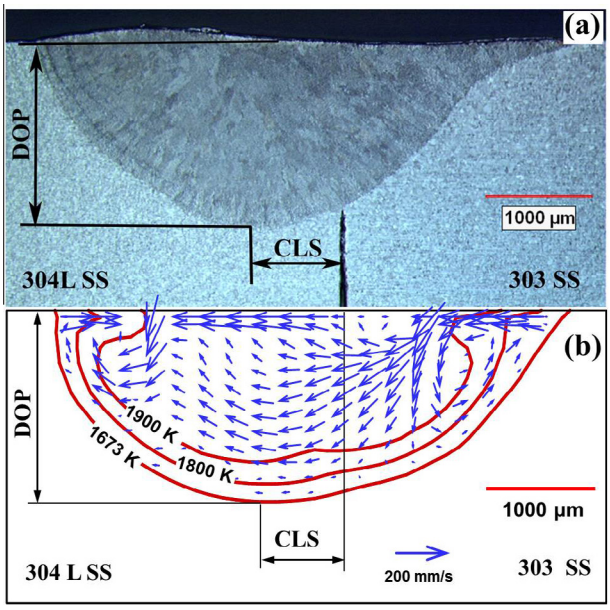

Fig. 1. Comparison of (a) etched transverse metallographic section reported by Lienert et al. [1] and (b) calculated weld cross section with temperature and velocity fields after 5.0 s. 304L SS plate contains 0.003 wt% sulfur and 303 SS plate contains 0.293 wt% sulfur. DOP indicates depth of penetration and CLS stands for center line shift.

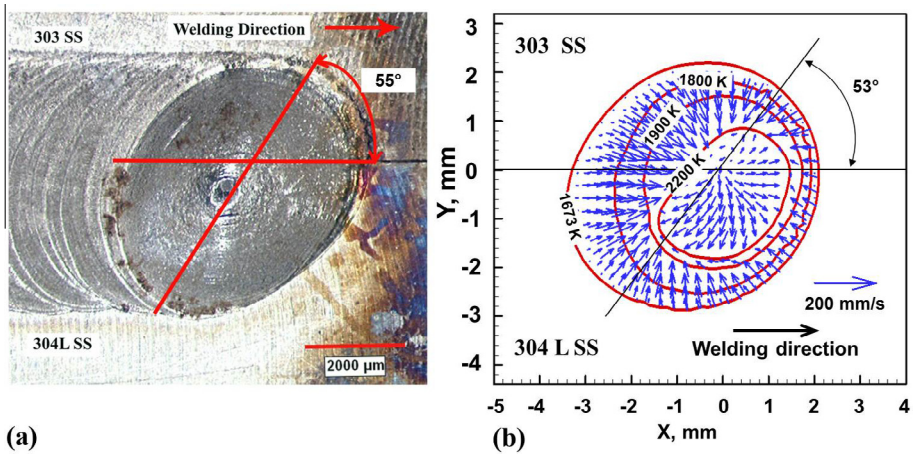

Fig. 2. Comparison of (a) macrograph of weld stop region reported by Lienert et al. [1] and (b) calculated weld pool profile of the top surface after 5.0 s. 304L SS plate contains 0.003 wt% sulfur and 303 SS plate contains 0.293 wt% sulfur.

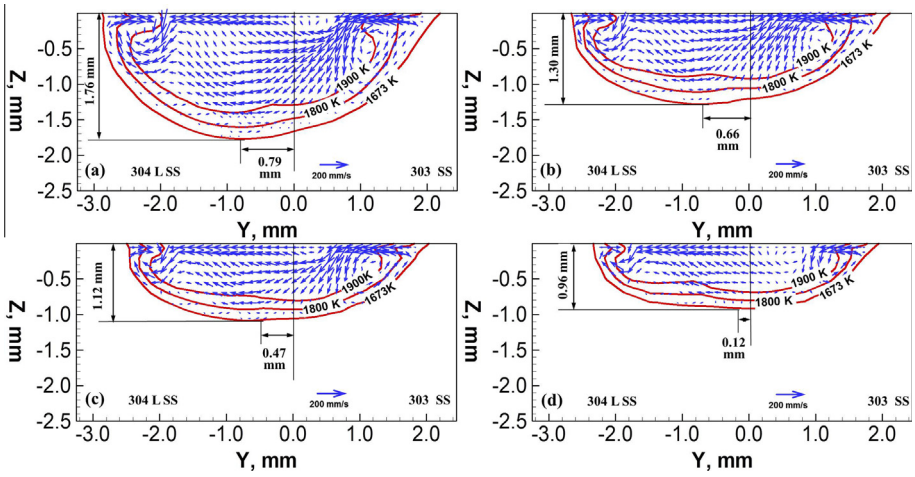

Fig. 3. Transverse sections of the simulated weld pool after 5.0 s for travel speeds of (a) 2.12 mm/s, (b) 3.12 mm/s, (c) 4.12 mm/s, and (d) 5.12 mm/s. 304L SS plate contains 0.003 wt% sulfur and 303 SS plate contains 0.293 wt% sulfur.

is formed with preferential melting of the low sulfur versus the high sulfur plate.

Fig. 2 demonstrates the top view of computed weld pool geometry and shows fair resemblance with the experimental weld stop region elliptical geometry. The major axis of simulated elliptical weld pool was found to be rotated about 53° from the welding direction along the line of joining, which is in good agreement with experimentally observed value, i.e., 55°. Both the experimentally determined and the computed results indicate significant preferential melting of lower sulfur work piece. The fair agreement between the computed and the experimental results of rotational asymmetry indicate that the rotation of weld pool takes place due to a superposition of surface driven fluid flow in the weld pool and its linear motion. Fig. 2(b) shows that on the weld pool surface, the liquid metal flows from the edge of the pool to its middle. This flow pattern results from the positive temperature coefficient of surface tension for 0.14 wt% sulfur for temperatures lower than about 2100 K. However, the temperature coefficient of surface tension is still negative for regions with temperature higher than 2100 K. So the fluid flow direction is outward inside the 2200 K isotherm.

As reported by Lienert et al. [1], the sulfur concentration determined by X-ray EDS characterization was fairly uniform throughout the fusion zone. Mishra et al. also reported [2] that for GTA welds of steels containing dissimilar concentrations of sulfur, there was no significant sulfur concentration gradient on the weld pool top surface as well as along the depth using electron probe microanalysis (EMPA) measurement. The reported homogenous distribution of sulfur throughout the weld was measured after the welding process. A significant sulfur composition difference which is 0.290 wt% exists at the beginning of welding. Therefore, there is a homogenization process for the sulfur distribution across the entire weld pool during welding. During this homogenization process, the sulfur concentration gradient is reduced with the sulfur concentration increasing on the low sulfur side and decreasing on the high sulfur side. However, the sulfur concentration on the high sulfur side is no lower than the low sulfur side throughout this entire process. Consequently, more heat is transported preferentially from the high sulfur to the low sulfur side because of the strong Marangoni stress induced fluid flow, and an asymmetric weld is obtained after the welding process is completed.

Fig. 3 shows the effect of welding speed on the computed weld transverse cross sections. The calculated depth of penetration and weld width decreases with the increase of welding speed. The preferential melting of the low sulfur stainless steel becomes less

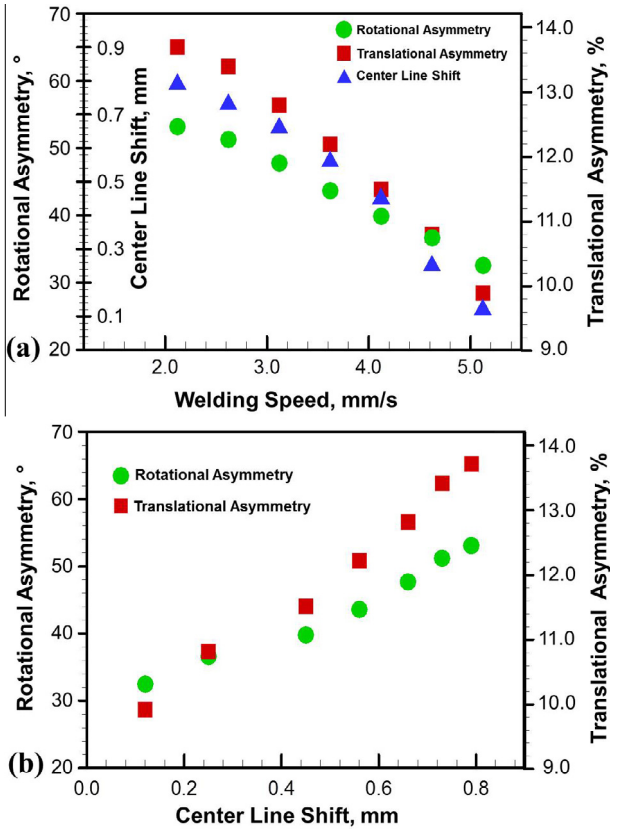

Fig. 4. Variation of computed results for (a) center line shift (CLS), rotational asymmetry (RA), and translational asymmetry (TA) with welding speed; (b) rotational asymmetry (RA) and translational asymmetry (TA) with center line shift (CLS).

obvious with increasing welding speed or decreasing heat input, which is consistent with the GTA welds reported by Mishra et al. [2]. The center line shift, rotational asymmetry and translational asymmetry values decrease as the welding speed increases from 2.12 to 5.12 mm/s as shown in Fig. 4(a). Fig. 4(b) shows the variation of rotational and translational asymmetry values with center line shift value, which indicates that the preferential melting of the plates below the weld surface can be evaluated from the observable rotational and translational asymmetry values. Thus, destructive tests can be avoided with direct measurement of the weld pool rotation angle or the high sulfur and low sulfur piece widths on the top surface.

In summary, the computed velocity fields show a net movement of liquid metal from the high sulfur 303 to the low sulfur 304L stainless steels. This motion results from Marangoni convection driven by spatial gradients of temperature and sulfur concentration, which causes a pronounced center line shift in linear welding. The rotational asymmetry of the weld pool results from the interaction between the velocity field in the weld pool driven by Marangoni convection and its linear motion. The extents of center line shift and translational asymmetry decrease with increase in travel speed. The mechanism of translational and rotational asymmetry proposed in this paper is consistent with experimental results of laser welding of dissimilar 303 and 304L stainless steels containing different concentrations of sulfur.

References

[1] T.J. Lienert, P. Burgardt, K.L. Harada, R.T. Forsyth, T. DebRoy, Scripta Mater. 71 (2014) 37.
[2] S. Mishra, T.J. Lienert, M.Q. Johnson, T. DebRoy, Acta Mater. 56 (2008) 2133.
[3] S.A. David, T. DebRoy, Science 257 (1992) 497.
[4] T. DebRoy, S.A. David, Rev. Mod. Phys. 67 (1995) 85.
[5] C.R. Heiple, J.R. Roper, Weld. J. 60 (8) (1981) 143s.
[6] C.R. Heiple, J.R. Roper, R.T. Stagner, J.J. Aden, Weld. J. 62 (3) (1983) 72s.
[7] W. Pitscheneder, T. DebRoy, K. Mundra, R. Ebner, Weld. J. 75 (3) (1996) 71s.
[8] W.S. Bennett, C.S. Mills, Weld. J. 53 (12) (1974) 548s.
[9] G.M. Oreper, T.W. Eagar, J. Szekely, Weld. J. 75 (3) (1983) 307s.
[10] A.F. Rollin, M.J. Bentley, Proceedings of the International Conference on the Effects of Residual, Trace and Microalloying Elements on Weldability and Weld Properties, The Welding Institute, Cambridge, 1984. p. 9.
[11] M.J. McNallan, T. DebRoy, Metal. Trans. B 22 (1991) 557.
[12] P. Sahoo, M.J. McNallan, T. DebRoy, Metal. Trans. B 19 (3) (1988) 483.
[13] S. Kou, D.K. Sun, Metal. Trans. A 16 (2) (1985) 203.
[14] K. Mundra, T. DebRoy, K.M. Kelkar, Numer. Heat Trans. 29 (1996) 115.
[15] W. Zhang, G. Roy, J. Elmer, T. DebRoy, J. Appl. Phys. 93 (2003) 3022.